

## Simulations to elucidate suprathermal deuterium ion tail observed in He<sup>3</sup> minority ICRF heated JET plasmas

F.S. Zaitsev<sup>1,a</sup>, A. Gondhalekar<sup>2</sup>, T.J. Johnson<sup>3</sup>, V.G. Kiptily<sup>2</sup>, S.E. Sharapov<sup>2,b</sup>,  
and JET EFDA contributors\*

*JET-EFDA, Culham Science Centre, Abingdon, OX14 3DB, UK*

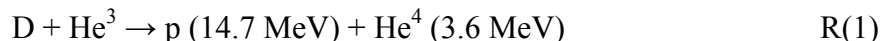
<sup>1</sup>*Moscow State University, Faculty of Computational Mathematics and Cybernetics, RF*

<sup>2</sup>*EURATOM/UKAEA Fusion Association, Culham Science Centre, Abingdon, OX14 3DB, UK*

<sup>3</sup>*Association EURATOM-VR, Royal Institute of Technology, 10044 Stockholm, Sweden*

<sup>a</sup>*e-mail: [zaitsev@cs.msu.su](mailto:zaitsev@cs.msu.su), <sup>b</sup>e-mail: [sergei.sharapov@jet.uk](mailto:sergei.sharapov@jet.uk)*

**1. Introduction:** Measurement and simulation of supra-thermal tail of the deuterium ion energy distribution produced during He<sup>3</sup> minority ICRF heating of deuterium plasmas in JET were reported in ref. [1]. The report demonstrated that the measured supra-thermal tail was an order of magnitude greater than that expected from model simulation of supra-thermal tail production due to Nuclear Elastic Scattering (NES) of Maxwellian deuterons on MeV energy ICRH driven He<sup>3</sup> ions alone. In ref. [1] we conjectured that the excess supra-thermal deuterium ion tail resulted from additional NES on MeV energy ions from the fusion reaction



The conjecture was reinforced by the inference, based on measurement of escaped energetic protons and He<sup>4</sup> ions [2], that a substantial population of (D + He<sup>3</sup>) fusion products was present in He<sup>3</sup> minority ICRF heated plasmas in JET, providing additional sources of NES. In ref. [1] we stressed the need to fully understand this JET observation, in view of the potential fusion boosting benefits of such processes in He<sup>3</sup> minority ICRF heated DT plasmas in ITER.

In this paper we describe *new* simulations of the previously reported [1] measurements of the supra-thermal tail of deuterium ion energy distribution function. A modified FPP-3D code, incorporating NES of Maxwellian D ions on the 3D steady state distributions of MeV energy ICRH driven minority He<sup>3</sup> ions, 14.7 MeV protons and 3.6 MeV He<sup>4</sup> ions from fusion reactions R(1) is presented. Using this we compute a line-of-sight integrated energy distribution function of the supra-thermal tail of deuterium ions for confrontation with measurements made using a Neutral Particle Analyzer (NPA) [1]. The complexity of the problem arises from having to simulate four simultaneously interacting ion species, D, He<sup>3</sup>, p, and He<sup>4</sup>, the strong anisotropy of ion distributions in phase space, large energy range and many kinetic effects such as large orbit widths, friction and diffusion in velocity, neoclassical radial transport, pitch angle scattering, fusion reactions, and NES.

The physical model and mathematical implementation of neoclassical transport in tokamak geometry in the FPP-3D Fokker Planck code has been described in detail in ref. [3]. The code uses as input the measured plasma equilibrium, measured parameters of the majority plasma species, and the energy distribution function of ICRF driven He<sup>3</sup> minority ions which was simulated using the SELFO Monte-Carlo code described in ref. [4].

**2. Experimental set-up and the line-of-sight integrated ion energy distribution function (LID) inferred from the NPA measurements:** The subject of simulation in this paper is the supra-thermal tail of the deuterium ion energy distribution function measured in JET pulse #53810 with He<sup>3</sup> minority ICRF heating of majority deuterium plasma. The tokamak equilibrium parameters were: toroidal magnetic field  $B_\phi(R_{mag}) \approx 3.45\text{T}$ , plasma current  $I_\phi \approx 1.8\text{MA}$ , major radius at the magnetic axis  $R_{mag} \approx 3 \text{ m}$ , plasma minor radius  $\gamma_a \approx 0.9 \text{ m}$ ,

\* See the Appendix of M.L. Watkins et al., Fusion Energy 2006 (Proc. 21st Int. Conf. Chengdu, 2006) IAEA, (2006).

elongation  $\varepsilon \approx 1.5$ . The plasma parameters, electron and ion densities, corresponding temperatures, minority He<sup>3</sup> ion density and other parameters were given previously in ref. [1]. The vertical NPA line-of-sight in JET was located at major radius  $R_{NPA} = 3.07$  m, close to the magnetic axis and the ICRH resonance layer. As described in refs. [5, 6] the deduced NPA line-of-sight integrated ion energy distribution function (LID) is that of trapped ions with pitch-angle  $\vartheta \approx \pi/2 \pm 5 \times 10^{-3}$  and with ion speeds ( $v_z/v_R$  and  $v_z/v_\phi$ )  $\geq 200$ , i.e. of ions at the tip of the banana orbits with speed directed towards the NPA. The NPA is of the conventional E||B type and therefore not able to distinguish between ions of the same mass/charge (A/Z) ratio, as described in ref. [5]. We point out that the new circumstance, presence of MeV energy He<sup>4</sup> ions from reaction R(1), requires that in inferring the LID of NES driven deuterium ions we have to correct for contamination by He<sup>4</sup> atomic flux to the NPA. We estimate that in for the measurements under consideration in the work described here the correction is negligible compared to the other uncertainties in the inferred LID of D ions.

**3. Data flow:** Figure 1 illustrates how the simulation was implemented. The geometry in FPP-3D was input from the measured plasma equilibrium. Since the measured LID of ICRH driven minority He<sup>3</sup> ions is a moment of the original 3D He<sup>3</sup> ion distribution function and thus can not be incorporated directly into FPP-3D, it was simulated using the SELFO code. To find the closest match between SELFO simulated and measured LID a scan over He<sup>3</sup>

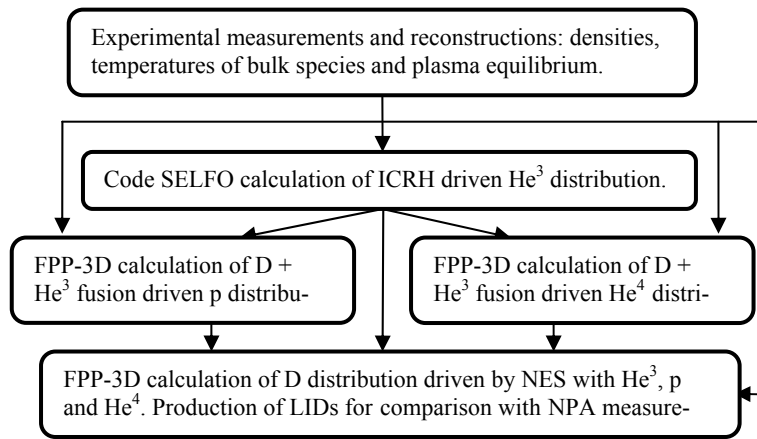


Figure 1. The flow of experimental and numerical data.

density, with 0.5, 1, 2 and 3 % of  $n_e$ , was performed. The best match was obtained with  $n_{He3}/n_e = 10^{-2}$ . The SELFO He<sup>3</sup> distribution function together with the measured plasma parameters were input into FPP-3D (fig. 1) to calculate the distribution functions of energetic protons and He<sup>4</sup> ions resulting from the fusion reaction R(1). Finally FPP-3D code was used again to calculate the supra-thermal tail of deuterium ion energy distribution function due to NES of Maxwellian deuterons on energetic He<sup>3</sup>, and protons and He<sup>4</sup> ions from the fusion reaction R(1) and hence the LID. The FPP-3D computation typically required  $\geq 45$  hours on a fast PC to obtain the energy distribution functions for fusion protons and He<sup>4</sup>, and the resulting tail of D ion energy distribution function.

**4. Result of simulations:** The comparison between the measured LID and simulated one is done at time  $t \geq 9.5$  s into the JET plasma pulse #53810. As discussed in ref. [1] at this time the measured plasma parameters  $T_e(0)$ ,  $T_i(0)$  and  $n_e(0)$  had reached steady state, indicating that the energy distribution functions of the MeV energy ions, ICRH driven He3 ions and protons and He4 ions from R(1), had all reached steady state. These features were tested and verified as part of the SELFO and FPP-3D simulations. This justifies using a model of steady state NES in the FPP-3D code, as described in ref. [1]. Fig. 2 shows the simulated LID of ICRH driven He<sup>3</sup> ions, LID of protons and He<sup>4</sup> ions from fusion reaction R(1), LID of supra-thermal tail of D ions due to NES on the He<sup>3</sup> alone, LID of supra-thermal tail of D ions due to combined NES on the He<sup>3</sup>, protons and He<sup>4</sup> ions, and lastly the experimentally determined LID of supra-thermal tail of D ions inferred from NPA measurements.

Supplementary FPP-3D calculations yielded that: (1) The fusion rate between ICRH driven He<sup>3</sup> ions and NES driven D ions was negligible compared to the fusion rate between

the much larger Maxwellian D ion population and the ICRH driven He<sup>3</sup>. Here we assumed a constant source of energetic He<sup>3</sup> ions due to ICRH, and neglected depletion of He<sup>3</sup> ions due to burn-up in fusion reaction R(1). (2) Of the two new projectile ion species considered, protons were the dominant NES driver of the supra-thermal tail of deuterium ion energy distribution function. This is because of the large cross-section for p→D NES shown in fig. 4 of ref. [1], and because of the mass factor  $\gamma^2$  in the source term in eq. (2) in ref. [1], where  $\gamma = (m_{target} + m_{projectile}) / (2m_{projectile})$ .

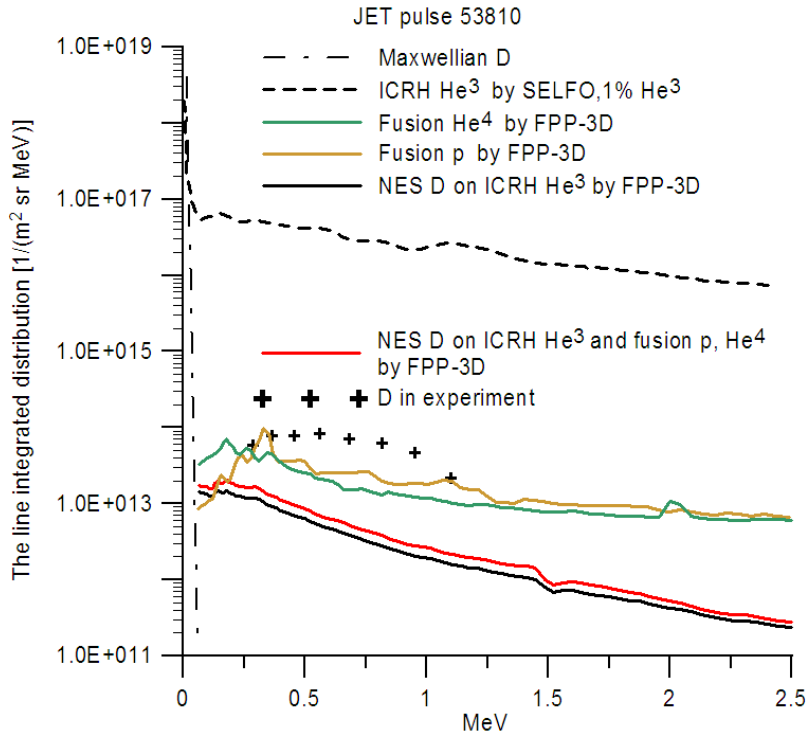


Figure 2: Measured and simulated LIDs at time  $t = 9.5s$ . The crosses show the LID of supra-thermal tail of deuterium ions inferred from the NPA measurements. Dashed curve shows the FPP-3D simulated LID of ICRH driven He<sup>3</sup> ions using the full 3D distribution function from the SELFO code. The solid black curve shows the FPP-3D simulated LID of supra-thermal tail of deuterium ions due to NES on He<sup>3</sup> ions alone, reported in ref. [1], showing the order of magnitude discrepancy between the measurement and simulation. The brown, green and red curves are the result of new simulations discussed in this paper. The brown and green curves are respectively FPP-3D simulations of LID of protons and He<sup>4</sup> ions from (D+He<sup>3</sup>) fusion reactions. The red curve shows the new FPP-3D simulation of the LID of supra-thermal tail of the deuterium ions

due to *combined effect* of NES on He<sup>3</sup> ions, and fusion protons and He<sup>4</sup> ions.

The fusion protons and He<sup>4</sup> ions are born in equal numbers and in the same spatial location. But the subsequent evolution of their distribution functions is determined by their different birth energies, masses, orbits, and slowing down kinetics. Fig. 1 shows a comparison between the resulting steady state LIDs of protons (brown curve) and He<sup>4</sup> ions (green curve).

Many FPP-3D runs were done to elucidate the “roughness” (local extrema) of the simulated LIDs of fusion protons and He<sup>4</sup> ions, and NES D ions. It was found that, depending on details of the SELFO simulation and physical model of kinetic processes used in FPP-3D, the roughness can be more or less pronounced or made to disappear. We stress however that the magnitude of the LIDs and its slope (“effective temperature”), in the range  $0.2 \geq E(\text{MeV}) \geq 1.5$ , remain roughly constant. The main factors which influence the roughness of the simulated LIDs are: (a) Details of the full 3D ion distribution functions. (b) Position of the NPA line-of-sight in relation to position of maximum of ICRH power deposition, the maximum of fusion p and He<sup>4</sup> source and the maximum of the D NES source term  $S$  in eq. (2) of ref. [1]. (c) Shape of energetic ion trajectories near the magnetic axis. (d) First orbit losses of fusion products to the wall. (e) Term  $\sqrt{E}$  in the expression for the LID in eq. (4) of ref. [1]. Existence or absence of the peak near 1MeV in the LIDs of protons, He<sup>4</sup> and He<sup>3</sup> ions is caused by overlapping of these factors.

Point (c) is illustrated in fig. 3, which presents the source of fusion protons and He<sup>4</sup> ions, showing that the maximum of the source, located at a position given by the normalized

flux  $\gamma/\gamma_a = 0.5$ , is displaced from the NPA line-of-sight. This behaviour is analogous to that of ICRH driven He<sup>3</sup> ions as shown in fig. 2 of ref.[1], and also fig. 5 of ref.[1]. All the factors mentioned above can give rise to artefacts in the simulated LIDs. However, these artefacts are small and do not impact inferences drawn from simulations of our measurements using SELFO and FPP-3D.

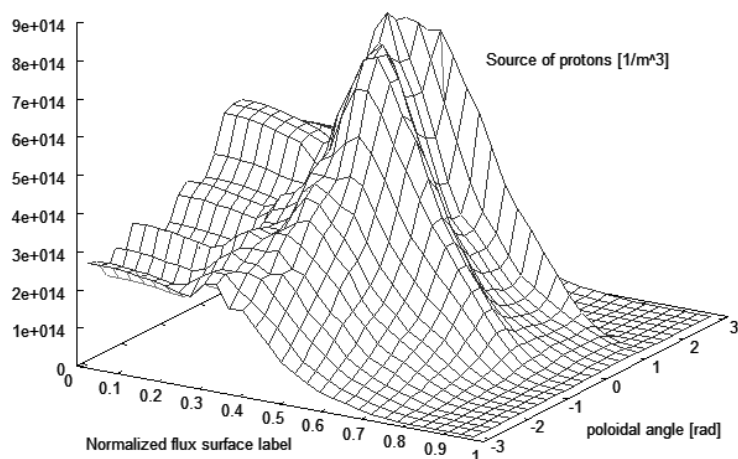


Figure 3. The birth profile of (D+He<sup>3</sup>) fusion protons, and by analogy of He<sup>4</sup> ions, per unit volume per second at poloidal angle  $\xi$  and normalized flux surface  $\gamma/\gamma_a$ , where  $\gamma_a$  corresponds to the plasma boundary.

**4. Conclusions:** The main conclusion from the *new* simulations incorporating NES of D target ions on all MeV energy projectile ions, namely ICRH driven He<sup>3</sup> ions, and protons and He<sup>4</sup> ions from the fusion reaction R(1), is that the (D+He<sup>3</sup>) fusion products make a contribution to the supra-thermal tail of D ion LID of nearly the same magnitude as the contribution of the primary ICRH driven He<sup>3</sup> ions alone. Protons, with their high energy and large cross-section for NES on D ions, are primarily responsible for this additional NES. The red curve in fig. 2 shows the case of 1% He<sup>3</sup> density as in ref. [1]. With higher He<sup>3</sup> density in the SELFO and FPP-3D the simulated NES driven supra-thermal tail of D ions can be increased in magnitudes and come closer to the measured LID, however such an increase in He<sup>3</sup> density can not at present be justified. We thus conclude that the excess in the measured LID of the supra-thermal tail of D ions, mentioned at the beginning of this paper as in ref. [1], has been only partially accounted for by NES on fusion protons and He<sup>4</sup> ions. The work described here to account for the observed excess of NES has yielded the important result that ions from the reaction R(1) are substantial drivers of additional NES of D ions in He<sup>3</sup> minority ICRH plasmas in JET. Efforts are in hand to clarify the source of the remaining measured excess, including re-examination of the experimental data and of uncertainties in the inferred LID, and critical re-examination of SELFO and FPP-3D code simulations.

**Acknowledgements:** Work at the UKAEA was jointly funded by the UK Engineering and Physical Sciences Research Council and by EURATOM. Work at MSU was partly funded by the Russian Foundation for Basic Research under grant N 07-07-00064.

**References:** [1] F.S. Zaitsev, et al., Plasma Physics and Control. Fusion. **49**(2007)1747. [2] V.G. Kiptily, et al., 10th IAEA Technical Meeting on Energetic Particles in Magnetic Confinement Systems, Germany, 2007, Paper IV-2. [3] F.S. Zaitsev, et al., Nuclear Fusion **42**(2002)1340. [4] Hedin J., Hellsten T., Eriksson L.-G. and Johnson T., Nuclear Fusion **42**(2002)527. [5] Korotkov A.A., Gondhalekar A. and Akers R.J., Phys. Plasmas **7**(2000)957. [6] Korotkov A.A., Gondhalekar A. and Stuart A.J., Nuclear Fusion **37**(1997)35.